PHYSICAL REVIEW B **94**, 100405(R) (2016)

Ab initio cycloidal and chiral magnetoelectric responses in Cr_2O_3

Natalie Tillack* and Jonathan R. Yates
Department of Materials, University of Oxford, Oxford OX1 3PH, United Kingdom

Paolo G. Radaelli
Department of Physics, University of Oxford, Oxford OX1 3PU, United Kingdom

(Received 2 March 2016; revised manuscript received 30 May 2016; published 28 September 2016)

We present a thorough density functional theory study of the magnetoelectric (ME) effect in Cr_2O_3. The spin-lattice ME tensor α was determined in the low-field and spin flop (SF) phases, using the method of dynamical magnetic charges, and found to be the sum of three distinct components. Two of them, a large relativistic "cycloidal" term and a small longitudinal term, are independent on the spin orientation. The third, only active in the SF phases, is also of relativistic origin and arises from magnetic-field-induced chirality, leading to a nontoroidal ME response.

DOI: 10.1103/PhysRevB.94.100405

The search for magnetoelectric (ME) materials, in which the electrical polarization P (the magnetization M) responds to the application of an external magnetic field H (electric field ϵ), has received a lot of attention in recent years [1–4], particularly in the context of "modern" multiferroic materials with a spontaneous polarization [5]. The linear magnetoelectric effect, whereby P is linearly proportional to H, is also of current technological interest for magnetic storage devices, replacements of superconducting quantum interference devices (SQUIDs), and the ME switching of exchange bias [6–8]. In the 1950's, Landau and Lifshitz were the first to demonstrate that the ME effect only occurs in magnetic (i.e., time-reversal odd) materials [9]. Cr_2O_3, often considered the prototypical ME, crystallizes in the trigonal corundum structure and, below the Néel temperature of $T_N = 307$ K, orders as a collinear antiferromagnet (AFM) with spins along the rhombohedral [111] direction (Fig. 1). Cr_2O_3 was predicted to be magnetoelectric based on symmetry considerations [10,11]—a prediction that was later verified experimentally [12–16]. Unlike most other MEs, Cr_2O_3 is ME above room temperature, making it technologically relevant in spite of the small ME response [17]. Cr_2O_3 is also ideal for studying the fundamental ME mechanisms, since it is not multiferroic, and—because of its magnetic point group—exhibits neither higher-order ME coupling nor piezomagnetism. Nevertheless, there is still a surprising amount of uncertainty surrounding the ME effect in Cr_2O_3, and in particular its behavior throughout the T-H phase diagram; in turns this hampers the systematic search for materials with a stronger ME response.

The linear ME coupling can be described by an axial tensor of rank two,

$$\alpha_{ij} = \left(\frac{\partial P_i}{\partial H_j}\right) = \mu_0 \left(\frac{\partial M_j}{\partial \epsilon_i}\right), \tag{1}$$

with $\mathbf{P}$ ($\mathbf{M}$) being the induced polarization (magnetization), $\mathbf{H}$ ($\boldsymbol{\epsilon}$) the external magnetic (electric) field, and μ_0 the magnetic permittivity. The components of P and H are conventionally expressed in a Cartesian coordinate system, with z along the rhombohedral [111] direction, x along one of the twofold axes, and y completing the right-handed set. The form of the linear ME tensor α_{ij} can be predicted entirely by symmetry once the AFM point group is known [18,19]. In low applied H [low-field (LF) phase], the Cr_2O_3 spins are aligned along z due to magnetic anisotropy [20,21] (magnetic point group $\bar{3}'m'$), making α_{ij} diagonal and α_{11} and α_{22} equal (Fig. 2). α_{33} is very small in the ground state, but becomes the dominant element at room temperature [22,23]. Under strong applied fields along z, Cr_2O_3 undergoes a first-order phase transition into the so-called *spin flop* (SF) phase, with spins ordered in the same G-type pattern, but directed in the basal plane [24] (middle panel in Fig. 1 [25]). The possible magnetic point groups of the SF phase, $2'/m$, $2/m'$, or $\bar{1}'$ for spins *parallel* or *perpendicular* to x or in a generic direction, respectively, also allow for the ME effect, but with a different, off-diagonal form of the ME tensor (see Fig. 2), which is indeed observed experimentally [26]. The ME effect in the SF phase has often been associated with the appearance of a *toroidal moment* $\boldsymbol{T} = \sum_i \mathbf{r}_i \times \mathbf{S}_i$ [26,27]. However, due to the presence of multiple domains in the SF phase (six domains are predicted, due the threefold symmetry breaking), it is unclear whether the ME tensor is purely toroidal (antisymmetric).

Here, we probe the ME effect in the LF and in the two high-symmetry SF phases ($2'/m$ and $2/m'$) in the ground state of Cr_2O_3 by a set of first-principles calculations—an approach that yields results that are fully consistent with experiments but avoids the domain problem. We demonstrate that the "large" components of the ME tensor in the SF phase are not intrinsically toroidal. Rather surprisingly, these components are numerically identical to the α_{11} and α_{22} tensor elements in the LF phase, clearly indicating a common origin. We further show that the signs and identical magnitudes of these "large" ME components can be predicted from the cycloidal spin-current mechanism, which is well known in multiferroics. Finally, we show that the "small" ME components in the SF phase arise from two separate mechanisms: a longitudinal response (e.g., α_{33} in the LF phase), which in the ground state is associated with a small longitudinal susceptibility of relativistic origin, whereas it becomes the dominant response at room temperature [28], and an additional chiral ME coupling.

*natalie.tillack@materials.ox.ac.uk

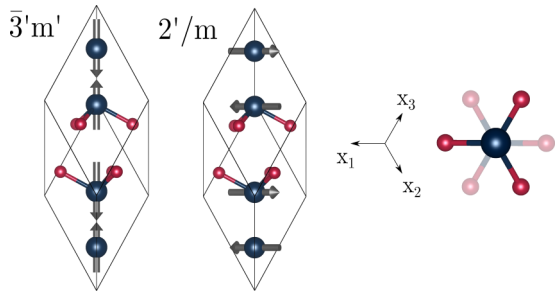

FIG. 1. Structures of Cr_2O_3. Left panel: Rhombohedral primitive cell of Cr_2O_3 with arrows indicating the AFM coupled Cr magnetic moments along z. The magnetic point group is $\bar{3}'m'$. Two 180° domains are possible, linked via time reversal. Middle panel: The spin flop state ($2'/m$ or $2/'m$), with spins aligned in the basal plane, thus breaking the threefold symmetry. Right panel: View along z (the half-transparent O atoms belong to the "lower" structural unit).

The ME response of Cr_2O_3 in the LF phase has been the subject of a number of first-principles studies [28–34]. The spin-lattice response $\boldsymbol{\alpha}^{\text{latt}}$ has been shown to be dominant [33], and we therefore focus on this contribution. We take the approach of Ref. [34] and expand the macroscopic response into microscopic quantities as follows,

$$\alpha_{kl}^{\text{latt}} = \frac{\partial P_k}{\partial H_l} = \left(\frac{\partial P_k}{\partial u_i}\right)\left(\frac{\partial u_i \partial u_j}{\partial E}\right)\left(\frac{\partial F_j}{\partial H_l}\right), \tag{2}$$

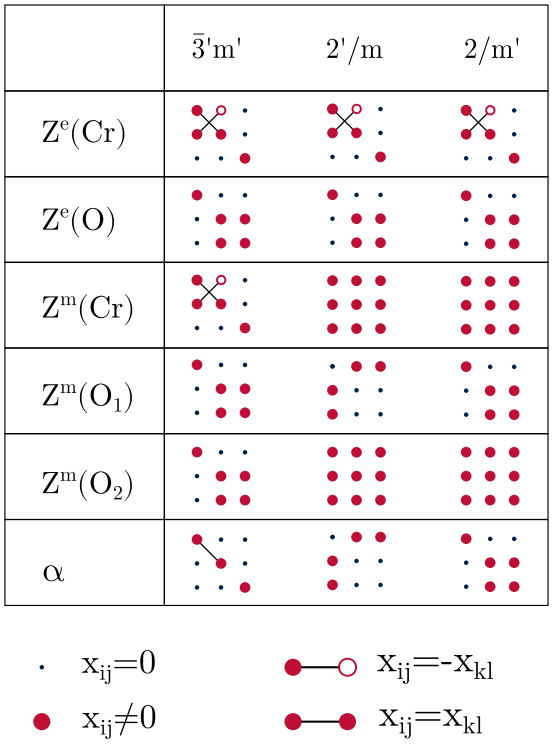

FIG. 2. Tensor forms of the BECs Z^e, magnetic charges Z^m (based on the atomic site symmetry), and of the overall ME coupling tensor α (based on the magnetic point group). In the low-field (spin flop) phase, the Wyckoff positions are $4c$ ($8f$) for the Cr atom, $6e$ ($4e$) for the O_1 atom, and $6e$ ($8f$) for the O_2 atom.

with the indices $k,l = 1,2,3$ and the composite indices (accounting for three directional dimensions and the number of atoms in the unit cell N) $i,j = 1,\ldots,3N$. Equation (2) shows a trilinear relation involving the Born effective charges (BECs) $Z^e_{ki} = \frac{\sigma}{e}\frac{\partial P_k}{\partial u_i} = -e\frac{\partial F_i}{\partial \epsilon_k}$, the inverse of the force-constant matrix $K^{-1}_{ij} = \frac{\partial u_i}{\partial F_j} = \frac{\partial u_i \partial u_j}{\partial E}$, and the dynamical magnetic charges (MCs). The latter can be understood as the magnetic analog of the BECs [29] and are defined as the derivative of the Hellman-Feynman forces with respect to a magnetic field, $Z^m_{jl} = \frac{\partial F_j}{\partial B_l} = \mu_0^{-1}\frac{\partial F_j}{\partial H_l}$, using $\mathbf{B} = \mu\mathbf{H} \approx \mu_0\mathbf{H}$ and the permeability (vacuum permeability) μ (μ_0) being $\mu \approx \mu_0$ in AFMs. The electronic ME contribution $\boldsymbol{\alpha}^{\text{el}}$ is calculated "directly" from Eq. (1) via the change in Berry phase polarization over H with fixed ionic positions [32].

We calculate the three contributions to Eq. (2) using density functional theory (DFT) within the local density approximation. We find that spin-orbit coupling (SOC) has a very small effect on the BEC and force-constant matrix (less than 1‰) and we therefore compute these quantities without SOC. This means that our BEC and force-constant matrix are the same in all three magnetic phases. In contrast, the MCs are a SOC-induced effect and we compute them using a noncollinear magnetism formalism employing SOC. A Zeeman magnetic field is applied according to Ref. [32] and the change in the ionic forces calculated. It is therefore the changes in the MCs which determine the differing form of $\boldsymbol{\alpha}^{\text{latt}}$ in the three magnetic phases. Full details of the DFT calculations, including an analysis of the influence of the choice of exchange-correlation functional, are provided in the Supplemental Material [35].

Our results for the LF $\bar{3}'m'$ phase were benchmarked against Ref. [34], leading to almost identical results. A full comparison to literature values is given in the Supplemental Material [35]. Table I shows our results for the magnetic charges for the LF $\bar{3}'m'$ phase with spins parallel to z, and the two SF phases, $2'/m$ and $2/m'$, with spins *parallel* and *perpendicular* to x, which is also the direction of the surviving twofold axis. Table II shows the overall lattice, electronic, and total ME response. The tensor forms for both quantities are in good agreement with our group theoretical analysis from Fig. 2. The ME coupling tensors are as predicted (bottom row of Fig. 2 and Table II) to within ± 0.001 ps m^{-1}, which we take to be our computational uncertainty.

The MCs in the $\bar{3}'m'$ phase are of the same form as the BEC tensors. Therefore, those phonon modes that couple to the electric field, i.e., the infrared (IR) active modes, are also the ones that couple to the magnetic field. In the $R\bar{3}c$ space group, the IR active modes are the doubly degenerate E_u modes, which are active in the xy plane, and the singly degenerate A_{2u} modes, active along z. Not including the acoustic modes, the Γ-centered IR active modes are therefore

$$\Gamma^{\text{IR}} = 4E_u + 2A_{2u}. \tag{3}$$

From a mode decomposition of the BECs and the MCs, we observe changes in the magnetoactive response when x and y are no longer equivalent. The degeneracy of the IR active E_u modes is removed, and other modes become magnetoactive in x,y, or z. We also find that the exceptionally large component in the Z^m(Cr)e (the 32 and 31 component in the $2'/m$ and

TABLE I. Magnetic charges Z^m ($10^{-2}\mu_B/\text{Å}$) for the LF and two SF phases of Cr_2O_3. The O_1 and O_2 positions in the $\bar{3}'m'$ phase are related by a threefold rotation and the Z^m given in the following table for comparison with the SF cases.

Phase	Z^m(Cr)	Z^m(O_1)	Z^m(O_2)
$\bar{3}'m'$	$\begin{pmatrix} 2.4 & 5.6 & 0.0 \\ -5.6 & 2.4 & 0.0 \\ 0.0 & 0.0 & 0.0 \end{pmatrix}$	$\begin{pmatrix} -2.8 & 0.0 & 0.0 \\ 0.0 & -0.5 & -0.0 \\ 0.0 & -2.7 & -0.0 \end{pmatrix}$	$\begin{pmatrix} -1.1 & 1.0 & 0.0 \\ 1.0 & -2.2 & 0.0 \\ 2.3 & 1.4 & 0.0 \end{pmatrix}$
$2'/m$	$\begin{pmatrix} 0.0 & -0.1 & -2.3 \\ 0.0 & 0.0 & 5.6 \\ 0.1 & 18.9 & 0.0 \end{pmatrix}$	$\begin{pmatrix} 0.0 & -1.5 & 3.0 \\ -0.3 & 0.0 & 0.0 \\ -0.1 & 0.0 & 0.0 \end{pmatrix}$	$\begin{pmatrix} 0.3 & 0.8 & 0.8 \\ 0.2 & -1.4 & -1.2 \\ -0.1 & -0.1 & -2.2 \end{pmatrix}$
$2/m'$	$\begin{pmatrix} -0.1 & 0.0 & -5.6 \\ 0.0 & 0.0 & -2.3 \\ -18.8 & 0.2 & 0.0 \end{pmatrix}$	$\begin{pmatrix} 1.7 & 0.0 & 0.0 \\ 0.0 & -0.3 & 0.1 \\ 0.0 & -0.1 & 2.5 \end{pmatrix}$	$\begin{pmatrix} -0.7 & 0.3 & -1.2 \\ 1.3 & 0.2 & 2.2 \\ -0.1 & -0.1 & -1.3 \end{pmatrix}$

$2/m'$ phase, respectively) maps onto magnetoactive modes that are mutually exclusive of the IR active ones. That value has therefore no effect on the coupling tensor. Even though the magnetic charge tensors are quite dissimilar, this leads to the rather surprising similarity of the coupling tensors. The full mode decomposition of the BECs and the MCs for the LF phase is given in the Supplemental Material [35].

On this basis, we make the following important observations. First, the ME tensor α is *not* what one would expect from a toroidal moment. There is clearly a toroidal (antisymmetric) component, but this is identical in magnitude to the traceless symmetric component. This should not be particularly surprising, since the toroidal mechanism $\mathbf{P} = \boldsymbol{T} \times \mathbf{H}$ does not capture the large difference between the longitudinal and transverse susceptibilities. Second, the magnitudes of the "large" elements of the ME tensor are the same (within error) in the two SF phases *and* in the LF phase. In fact, all these large elements of the total ME response (italics in Table II) can be approximated by the following compact expression,

$$\boldsymbol{\alpha}^{\text{tot}} \approx 0.8\ \text{ps}\,\text{m}^{-1} \begin{pmatrix} \hat{m}_z & 0 & -\hat{m}_x \\ 0 & \hat{m}_z & -\hat{m}_y \\ 0 & 0 & 0 \end{pmatrix}, \tag{4}$$

where $\hat{m}_x$, $\hat{m}_y$, and $\hat{m}_z$ are the components of a unit vector parallel to the spin on the Cr(4*c*) atom at Wyckoff position 0.1590. A clue as to the origin of this tensor form is the fact that all these components correspond to a *transverse* spin response in the plane containing both the spins and z, so that the rotated spins under the action of the magnetic field can be thought as forming a segment of a cycloid. Here below, we show that the tensor form in Eq. (4) is exactly the one predicted from the spin current [36] or inverse Dzyaloshinskii-Moriya (DM) [37] mechanisms, which are well known in the context of multiferroics. We write the transverse response of the magnetization $\mathbf{m}_i$ on Cr site i as

$$\Delta\mathbf{m}_i = \chi^T \frac{\mathbf{m}_i \times (\mathbf{H} \times \mathbf{m}_i)}{m^2} = \chi^T \left(\mathbf{H} - \frac{\mathbf{m}_i (\mathbf{H} \cdot \mathbf{m}_i)}{m^2} \right), \tag{5}$$

where χ^T is the transverse susceptibility. The inverse DM polarization is

$$\begin{aligned} \mathbf{P} &= \mu \mathbf{r}_{12} \times (\mathbf{m}_1 \times \mathbf{m}_2) = 2\mu \chi^T \mathbf{r}_{12} \times (\mathbf{m} \times \mathbf{H}) \\ &= 2\mu \chi^T (\mathbf{m}(\mathbf{H} \cdot \mathbf{r}_{12}) - \mathbf{H}(\mathbf{m} \cdot \mathbf{r}_{12})) \end{aligned} \tag{6}$$

TABLE II. Lattice, electronic, and total ME coupling tensor α (ps m^{-1}) for the LF and two SF phases of Cr_2O_3. Italics describe the transverse terms due to the DM interaction. The bold terms in the SF phases are the transverse in-plane responses, which are attributed to chiral coupling.

Phase	α^{latt}	α^{el}	α^{tot}
$\bar{3}'m'$	$\begin{pmatrix} \textit{0.310} & 0.000 & -0.001 \\ 0.000 & \textit{0.310} & 0.000 \\ 0.000 & 0.000 & 0.005 \end{pmatrix}$	$\begin{pmatrix} \textit{0.525} & 0.000 & -0.001 \\ 0.000 & \textit{0.525} & 0.000 \\ 0.000 & 0.000 & 0.000 \end{pmatrix}$	$\begin{pmatrix} \textit{0.835} & 0.000 & -0.001 \\ 0.000 & \textit{0.835} & 0.000 \\ 0.000 & 0.000 & 0.005 \end{pmatrix}$
$2'/m$	$\begin{pmatrix} -0.001 & \mathbf{-0.012} & \textit{-0.309} \\ 0.001 & -0.001 & 0.000 \\ 0.019 & 0.000 & 0.000 \end{pmatrix}$	$\begin{pmatrix} 0.000 & \mathbf{-0.028} & \textit{-0.518} \\ 0.000 & 0.000 & 0.000 \\ 0.062 & 0.000 & 0.000 \end{pmatrix}$	$\begin{pmatrix} -0.001 & \mathbf{-0.040} & \textit{-0.827} \\ 0.001 & -0.001 & 0.000 \\ 0.081 & 0.000 & 0.000 \end{pmatrix}$
$2/m'$	$\begin{pmatrix} \mathbf{-0.012} & 0.000 & 0.000 \\ 0.000 & -0.002 & \textit{-0.309} \\ 0.000 & 0.019 & 0.001 \end{pmatrix}$	$\begin{pmatrix} \mathbf{-0.028} & 0.000 & 0.000 \\ 0.000 & 0.000 & \textit{-0.518} \\ 0.000 & 0.062 & 0.000 \end{pmatrix}$	$\begin{pmatrix} \mathbf{-0.040} & 0.000 & 0.000 \\ 0.000 & -0.002 & \textit{-0.827} \\ 0.000 & 0.081 & 0.001 \end{pmatrix}$

where μ is a coupling constant and, in the case of Cr_2O_3, $\mathbf{r}_{12} \parallel c$. With this, the ME tensor takes the form

$$\begin{aligned}\boldsymbol{\alpha} &= 2\mu\chi^T(\mathbf{m}\otimes\mathbf{r}_{12} - \mathbf{m}\cdot\mathbf{r}_{12}\mathbb{1}) \\ &= -2\mu\chi^T\begin{pmatrix} m_z & 0 & -m_x \\ 0 & m_z & -m_y \\ 0 & 0 & 0 \end{pmatrix},\end{aligned} \tag{7}$$

where $\otimes$ is the outer (tensor) product and $\mathbb{1}$ is the unit tensor. Equations (7) and(4) have exactly the same form, including the nontrivial sign of the tensor elements.

In all phases, the ME tensor α has a small longitudinal term (i.e., with the field H parallel to the spins) of magnitude 0.005 ps m^{-1} (0.081 ps m^{-1}) for the LF (SF) phase(s), which generates $P \parallel z$ in all cases. In the ground state, this is associated with a small longitudinal susceptibility of relativistic origin, while at finite temperatures, the symmetric Heisenberg exchange makes this term become the dominant contribution to α in the LF phase, as shown in Ref. [28].

Considerably more interesting is the additional *in-plane transverse* term of magnitude -0.040 ps m^{-1}, which is only present in the SF phases. Here, the field H lies in the xy plane perpendicular to the spins and generates $P \parallel x$, i.e., to the surviving twofold axis of the monoclinic structure. Phenomenologically, this term is associated with a *fifth-order* invariant of the form $(m_x^2 - m_y^2)A_x - 2m_x m_y A_y$ where $\mathbf{A} = (m_y H_x - m_x H_y)\mathbf{P}$ transforms as an axial (parity-even) vector. In the remainder, we show that this term is due to the breaking of axial symmetry upon SF magnetic ordering, coupled with the breaking of chiral symmetry upon application of a magnetic field in the in-plane transverse direction.

As we already mentioned, SF magnetic ordering breaks the threefold symmetry. Consequently, the *crystallographic* symmetry is also lowered, due to coupling of the staggered magnetization with a structural order parameter, which has the transformation properties of an axial vector $\mathbf{A}$. Minimizing the Landau free energy with respect to $\mathbf{A}$ in the usual way, one obtains

$$\begin{aligned} A_x &= \lambda\left(m_x^2 - m_y^2\right), \\ A_y &= -\lambda(m_x m_y), \end{aligned} \tag{8}$$

where λ is a (small) magnetoelastic coupling constant. It is noteworthy that $A_y = 0$ in both of the SF phases we considered, so $\mathbf{A}$ is directed along x. Upon application of a magnetic field in the in-plane transverse direction, the rotated spins can be thought as forming a segment of a helix, which has the distinct chirality $\mathbf{r}_{12}\cdot(\mathbf{m}_1\times\mathbf{m}_2)$. In analogy to the ferroaxial multiferroic mechanism [38,39], we can therefore write the following phenomenological polarization,

$$\begin{aligned} P_x &= \mu\lambda\left(m_x^2 - m_y^2\right)\mathbf{r}_{12}\cdot(\mathbf{m}_1\times\mathbf{m}_2) \\ &= 2\mu\chi^T\lambda\left(m_x^2 - m_y^2\right)\mathbf{r}_{12}\cdot(\mathbf{m}\times\mathbf{H}) \\ &= 2\mu\chi^T\lambda\left(m_x^2 - m_y^2\right)(\mathbf{r}_{12}\times\mathbf{m})\cdot\mathbf{H}, \quad P_y = 0, \end{aligned} \tag{9}$$

yielding

$$\boldsymbol{\alpha} = 2\mu\chi^T\lambda\left(m_x^2 - m_y^2\right)\hat{\mathbf{x}}\otimes(\mathbf{r}_{12}\times\mathbf{m}), \tag{10}$$

where $\hat{\mathbf{x}}$ is a unit vector along x. Since $(\mathbf{r}_{12}\times\mathbf{m}) = (-m_y, m_x, 0)$, the ME tensor has the desired form

$$\boldsymbol{\alpha} = -2\mu\chi^T\lambda m^2\begin{pmatrix} m_y & m_x & 0 \\ 0 & 0 & 0 \\ 0 & 0 & 0 \end{pmatrix}, \tag{11}$$

which corresponds to the first-principles result (bold font in Table II). By comparing Eq. (11) with Eq. (7), one can understand why the former, containing the small parameter λ, is considerably smaller than the latter.

In summary, we have computed the magnetoelectric tensor of Cr_2O_3 in both low-field and high-field (spin flop) phases by means of first-principles calculations. We find that the ME tensor is not primarily toroidal, as previously speculated. Instead, its approximate form can be well predicted phenomenologically using the spin-current model, which is well known in multiferroics. There are two additional small components: The first is a longitudinal component known from previous studies of the low-field phase, while the second arises from a different chiral mechanism, which is akin to the ferroaxial mechanisms in multiferroics.

The work done at the University of Oxford was funded by EPSRC Grants No. EP/J003557/1, entitled "New Concepts in Multiferroics and Magnetoelectrics," and No. EP/M020517/1, entitled "Oxford Quantum Materials Platform Grant," the Scatcherd European Scholarship (N.T.), and The Royal Society (J.R.Y.). This work used the ARCHER UK National Supercomputing Service (http://www.archer.ac.uk), for which access was obtained via the UKCP consortium and funded by EPSRC Grant Ref. EP/K013564/1. We are also grateful for many valuable discussions with M. Ye and D. Vanderbilt.

[1] H. Schmid, Ferroelectrics **162**, 317 (1994).
[2] M. Fiebig, J. Phys. D **38**, R123 (2005).
[3] S.-W. Cheong and M. Mostovoy, Nat. Mater. **6**, 13 (2007).
[4] J. F. Scott, J. Mater. Chem. **22**, 4567 (2012).
[5] W. Eerenstein, N. D. Mathur, and J. F. Scott, Nature (London) **442**, 759 (2006).
[6] M. Fiebig and N. A. Spaldin, Eur. Phys. J. B **71**, 293 (2009).
[7] P. Borisov, A. Hochstrat, X. Chen, W. Kleemann, and C. Binek, Phys. Rev. Lett. **94**, 117203 (2005).
[8] P. Borisov, A. Hochstrat, V. V. Shvartsman, and W. Kleemann, Rev. Sci. Instrum. **78**, 106105 (2007).
[9] L. D. Landau and E. M. Lifshitz, *Electrodynamics of Continuous Media* (Pergamon, Oxford, UK, 1960).
[10] I. Dzyaloshinsky, J. Phys. Chem. Solids **4**, 241 (1958).
[11] I. E. Dzyaloshinskii, Sov. Phys. JETP **10**, 628 (1960).
[12] D. N. Astrov, Sov. Phys. JETP **11**, 708 (1960).
[13] D. N. Astrov, Sov. Phys. JETP **13**, 729 (1961).
[14] V. J. Folen, G. T. Rado, and E. W. Stalder, Phys. Rev. Lett. **6**, 607 (1961).
[15] G. T. Rado, Phys. Rev. **128**, 2546 (1962).
[16] G. T. Rado and V. J. Folen, J. Appl. Phys. **33**, 1126 (1962).

[17] M. Street, W. Echtenkamp, T. Komesu, S. Cao, P. A. Dowben, and C. Binek, Appl. Phys. Lett. **104**, 222402 (2014).
[18] H. Wiegelmann, A. G. M. Jansen, P. Wyder, J.-P. Rivera, and H. Schmid, Ferroelectrics **162**, 141 (1994).
[19] A. S. Borovnik-Romanov and H. Grimmer, in *International Tables for Crystallography*, Vol. D (Wiley, Hoboken, NJ, 2006), Chap. 1.5, pp. 105–149.
[20] J. W. Allen, Phys. Rev. B **7**, 4915 (1973).
[21] M. R. J. Gibbs, *Modern Trends in Magnetostriction Study and Application* (Springer, Berlin, 2001), p. 242.
[22] E. Kita, K. Siratori, and A. Tasaki, J. Appl. Phys. **50**, 7748 (1979).
[23] A. Scaramucci, E. Bousquet, M. Fechner, M. Mostovoy, and N. A. Spaldin, Phys. Rev. Lett. **109**, 197203 (2012).
[24] J. Ohtani and K. Kohn, J. Phys. Soc. Jpn. **53**, 3744 (1984).
[25] K. Momma and F. Izumi, J. Appl. Crystallogr. **44**, 1272 (2011).
[26] Y. F. Popov, A. M. Kadomtseva, D. V. Belov, and G. P. Vorob, J. Exp. Theor. Phys. Lett. **69**, 330 (1999).
[27] N. A. Spaldin, M. Fiebig, and M. Mostovoy, J. Phys.: Condens. Matter **20**, 434203 (2008).
[28] M. Mostovoy, A. Scaramucci, N. A. Spaldin, and K. T. Delaney, Phys. Rev. Lett. **105**, 087202 (2010).
[29] J. Íñiguez, Phys. Rev. Lett. **101**, 117201 (2008).
[30] S. Coh, D. Vanderbilt, A. Malashevich, and I. Souza, Phys. Rev. B **83**, 085108 (2011).
[31] E. Bousquet and N. A. Spaldin, Phys. Rev. Lett. **107**, 197603 (2011).
[32] E. Bousquet, N. A. Spaldin, and K. Delaney, Phys. Rev. Lett. **106**, 107202 (2011).
[33] A. Malashevich, S. Coh, I. Souza, and D. Vanderbilt, Phys. Rev. B **86**, 094430 (2012).
[34] M. Ye and D. Vanderbilt, Phys. Rev. B **89**, 064301 (2014).
[35] See Supplemental Material at http://link.aps.org/supplemental/10.1103/PhysRevB.94.100405 for computational details and comparison to literature values of ME and ground-state properties.
[36] H. Katsura, N. Nagaosa, and A. V. Balatsky, Phys. Rev. Lett. **95**, 057205 (2005).
[37] M. Mostovoy, Phys. Rev. Lett. **96**, 067601 (2006).
[38] R. D. Johnson, S. Nair, L. C. Chapon, A. Bombardi, C. Vecchini, D. Prabhakaran, A. T. Boothroyd, and P. G. Radaelli, Phys. Rev. Lett. **107**, 137205 (2011).
[39] R. D. Johnson, L. C. Chapon, D. D. Khalyavin, P. Manuel, P. G. Radaelli, and C. Martin, Phys. Rev. Lett. **108**, 067201 (2012).